Appl Magn Reson (2016) 47:1003–1014
DOI 10.1007/s00723-016-0803-7

Applied
Magnetic Resonance

Identification of Free Radicals Generated by Different Curing Modes in a Dental Resin Cement

Bruno Luiz Santana Vicentin[1] · Antonio Marchi Netto[2] · Bernhard Blümich[2] · Eduardo Di Mauro[1]

Received: 23 April 2016 / Revised: 10 June 2016 / Published online: 24 June 2016
© Springer-Verlag Wien 2016

Abstract The polymerization process of the dual cure resin cement AllCem (FGM, Joinvile, Brazil) was investigated theoretically and experimentally. The free radicals responsible for polymerization continuity were characterized by multi-frequency EPR spectroscopy (X-, Q- and W-band) and spectra simulation. It was observed by multifrequency electron paramagnetic resonance spectroscopy and spectra simulation that the paramagnetic species occur simultaneously and independently for both self-cure and photo-cure modes. The paramagnetic species generating the EPR signal are the same for both photo-cure and self-cure polymerization mechanisms.

1 Introduction

In clinical situations of extensive coronary destruction the use of a retentive system for the tooth restorative material is required [1]. The post-and-core technique currently is the recommended protocol in tooth restoration to cement the post into the root canal. Methyl Methacrylate (MMA)-based polymers have been widely used in dental and orthopedic applications, although Poly(Methyl Methacrylate) (PMMA) based materials are thermoplastic, viscous materials with limited strength [2]. The clinical results improved with the use of systems based on dymethacrylate monomers. The most important dymethacrylate is Bis-phenol-A-bis(glycidyl methacrylate) (Bis-GMA), which copolymerizes with triethylene glycol dimethacrylate (TEGDMA). Also the dimethacrylate monomers Bis-phenol-A-dimethacrylate (Bis-EMA) and a urethane

✉ Bruno Luiz Santana Vicentin
bruno.vicentin@uel.br

[1] Department of Physics, State University of Londrina, Rodovia Celso Garcia Cid PR-445 km 380, Londrina 86057-970, Brazil

[2] Institute of Technical and Macromolecular Chemistry, RWTH Aachen University, Aachen, Germany

dimethacrylate (UDMA) are commonly used [2]. Dimethacrylate monomer based materials polymerize at room temperature following photoinitiation, where the photoinitiation system is the combination of camphoroquinone (CQ) with amine to produce Free Radicals (FRs), or they polymerize by redox initiation in a combination of benzoyl peroxide (BPO) with N,N-dimethyl-p-toluidine (DMT) [3, 4]. Because of clinical implications, an inhibitor is also added in the composition to guarantee that the material will not polymerize during storage and to provide the necessary working time to the professional.

In the post cementation procedure, the root canal is filled with resin cement and thus the post is introduced into the canal keeping a small part of it out of the root canal to perform the external restoration [4, 5]. Later, the system is irradiated for $\sim$40 s to polymerize (cure) the resin cement. As the polymerization of the cement takes place inside the root canal the post is usually translucent for the purpose of conducting light to the deepest points of the canal [1, 2]. The efficiency of the retention of the translucent fiberglass post inside the treated canal is essential for the quality of the restoration. The bonding material should have excellent biocompatibility [6] and proper physical and mechanical properties [7–9] to prevent potentially early restoration failure [10, 11].

The polymerization degree is fundamental to the retention of the post and is related to the amount of free radicals (FRs) generated in the initiation stage of the polymerization reaction [12, 13]. The capability of the translucent post to conduct light to the deepest points of the root canal have been studied, and the results showed that in the apical and profound parts the photo-cure is not effective, so that the resin cement remains unpolymerized, compromising the final result of the restoration [14, 15]. To guarantee that the cement gets polymerized in all the extension of the post, dual cure resin cements have been developed associating light irradiation (photo-cure) to chemical initiation (self-cure), ensuring polymerization at deepest points of the restoration where radiation cannot excite camphoroquinone [16, 17].

The photopolymerizable dental resin have been widely studied to determine their polymerization kinetics [18–20], the free radicals responsible for the initiation of chain reaction [21, 22], and irradiation protocols [23]. But some questions about the resin cement used for post fixation remain unsolved. This research was conducted to identify the free radicals responsible for the chain reaction. X-, Q- and W-band electron paramagnetic resonance (EPR) spectroscopy and spectra simulation were used to identify the free radicals responsible for continuing the polymerization [21].

2 Experimental

2.1 Materials

Samples of dual cure resin cement from Allcem (FGM, Joinville, Brazil) in the color shade A1 were examined by X-, Q- and W-bands EPR. The initial compounds are two pastes separated in a dual body syringe which are mixed in a self-mixing nozzle that accompanies the kit. The polymerization reaction begins upon mixing the base

paste with the catalyst in the nozzle, and it can be accelerated by blue light irradiation. In all experiments the initial paste and catalyst were mixed in a 1:1 weight ratio. The particular resin cement was chosen for this study because it has the same composition and showed similar properties and quality compared to others used worldwide for the purpose of translucent fiberglass post cementation. The irradiation of the cement with the blue visible light was produced by a LED (Ultra Blue, Dabi Atlante, Ribeirão Preto, Brazil) with a potency of 492 mW/cm^2. The resin cement samples were separated in two major groups: irradiated for 40 s and not-irradiated. Multifrequency EPR spectroscopy aims at improving the spectroscopic information from the use of different field strengths [21].

2.2 Electron Paramagnetic Resonance (EPR)

The X-band ($\sim$9 GHz) EPR spectra were obtained with a JEOL JES-PE-3X spectrometer at room temperature using 1 mW microwave power, 0.40 mT modulation amplitude, and 100 kHZ modulation frequency to avoid signal saturation. The samples were placed in a 2 $\times$ 2 mm Teflon mold. The Q-band EPR spectra were obtained with a Bruker ER-5106 QT spectrometer at 0.5 mW microwave power and 0.40 mT modulation amplitude. The samples were placed in a 1 $\times$ 1 mm Teflon mold. The W-band EPR spectra were obtained with a Bruker Elexsys E 680 spectrometer fitted with a TerraFlex probe, with samples dimensions of less than 1 mm. All experiments were carried out at room temperature. The data treatment was performed with OriginLab software, and simulations were achieved using the WinEPR (Bruker) software.

3 Results and Discussions

3.1 Polymerization Mechanisms

A polymerization reaction encompasses three stages: initiation, propagation and termination. In the initiation stage the reaction is started by generating free radicals, and these radicals react with first monomer. In the propagation stage successive reactions with monomers occurs until the reaction is terminated, typically by combination of monomers or disproportionation. Consider R* being a primary radical (generated by a redox reaction or blue visible light irradiation) and M the monomer molecule. The general reaction mechanism for the free radical polymerization with termination by combination of monomer is as follows [18]:

Initiation:

$$R^* + M \xrightarrow{k_i} RM_1^* \tag{1}$$

Propagation:

$$RM_1^* + M \xrightarrow{k_p} RM_2^* \tag{2}$$

$$RM_2^* + M \xrightarrow{k_p} RM_3^* \quad (3)$$

$$RM_x^* + M \xrightarrow{k_p} RM_{x+1}^* \quad (4)$$

Termination:

$$RM_n^* + RM_m^* \xrightarrow{k_t} RM_{m+n}R \quad (5)$$

In these reactions k_i, k_p and k_t denote the reaction rate constants of the initiation, propagation and termination stages, respectively [18].

In the self-cure process the BPO is degraded releasing two primary radicals and an inert product [24]. Figure 1 represents the BPO degradation by interaction with the tertiary amine 4-(N, N-dimethylamine) phenetyl alcohol (DMPOH) [24]. The primary free radicals generated in the self-cure are the N-methylene radical (named PRI) and the benzoyloxy radical (named PRII), while the inert product is benzoic acid [24]. Subsequently, PRI and PRII react with monomers leading to the induction step and then to the propagation step, where the active monomer reacts with another monomer molecules. The PRI reacts with monomers by breaking the double bonding or by hydrogen abstraction (Figs. 2, 3). The reaction generates two different radicals, the propagating radical (RI) and the allylic radical (RII), which can be detected by EPR spectroscopy. Figures 4 and 5 represent the reaction of the PRII with methacrylate monomer generating two different radicals, RIII and RII.

In addition to the self-cure, the dual cure resin cement has the photo-cure initiators added to its composition. The photoinitiation mechanism by the camphoroquinone reaction with a tertiary amine is well described by Truffier-Boutry et al. [22] for the composite resin. As the EPR spectrum does not depend on

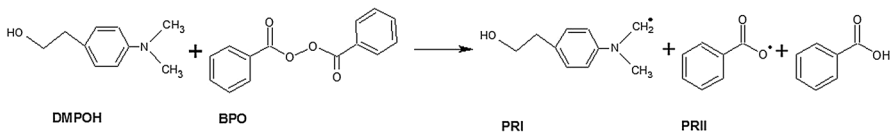

Fig. 1 Degradation process of BPO generating two primary radicals, PRI (N-methylene radical) and PRII (benzoyloxy radical), and one inert product

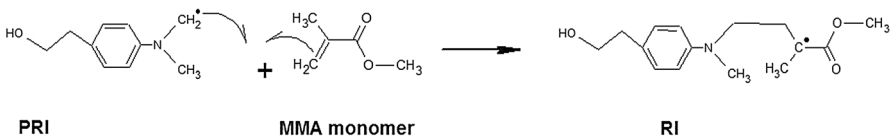

Fig. 2 Reaction of PRI with a MMA monomer generating the propagating radical (RI)

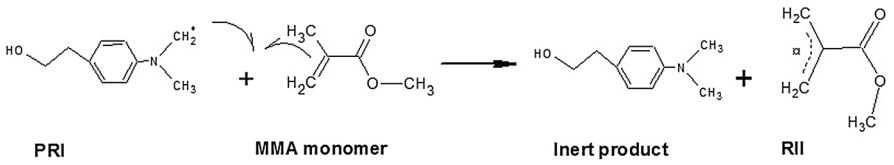

Fig. 3 Reaction of PRI with a MMA monomer by hydrogen abstraction generating an inert product and an allylic radical (RII)

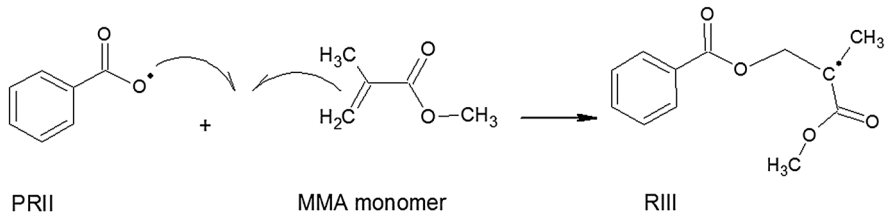

Fig. 4 Reaction of PRII with a MMA monomer generating the propagating radical (RIII)

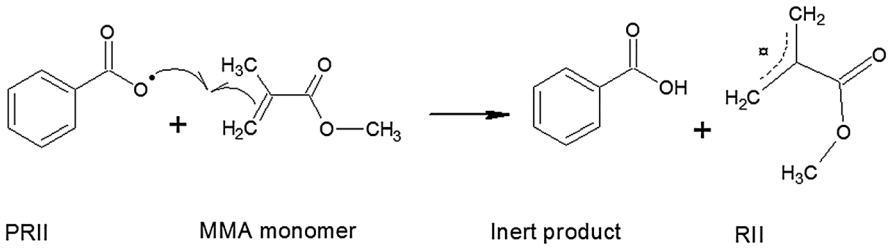

Fig. 5 Reaction of PRII with a MMA monomer by hydrogen abstraction generating an inert product and an allylic radical (RII)

the inorganic charges and the self-cure takes place independently of the photo-cure, the model proposed by Truffier-Boutry et al. [21] is applicable to this case, such that the free radicals responsible for the continuity of the polymerization initiated by photo-cure are the propagating (CH3-C*-CH2) and the allylic (CH2-C*-CH2) radicals, as shown by Fontes et al. [21]. Since no EPR spectroscopy data about curing of self-cure/dual-cure dental materials were available, it was performed multi-frequency EPR (X-, Q- and W-band) measurements to analyze changes in the spectra considering the two initiation mechanisms.

3.2 Multi-Frequency EPR Experiment

For mobile radicals the radical structures RI, RII, RIII are assumed. It is possible to see that the unpaired electrons in RI and RIII have the same neighborhood (CH3-C*-CH2), while RII has the CH2-C*-CH2 structure for the closest neighbors. These radicals are the same as the free radicals discussed by Truffier-Boutry et al. [22] to

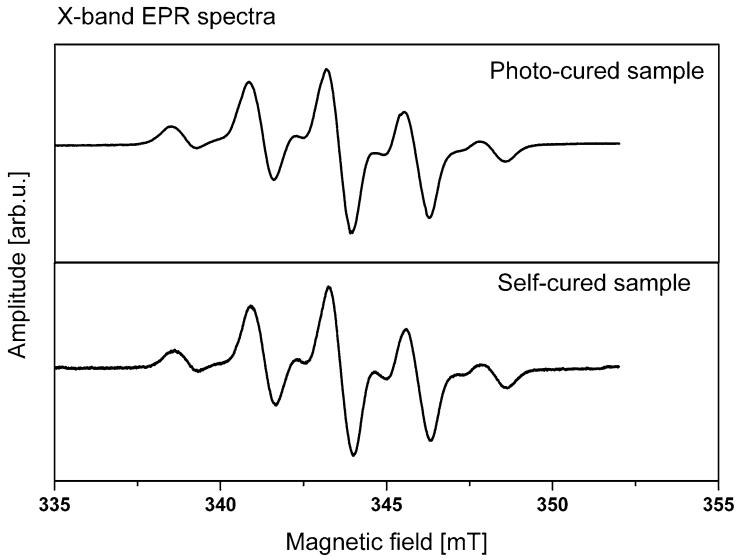

Fig. 6 X-band EPR spectra for the photo-cured and the self-cured samples of the dual cure resin cement AllCem

be responsible for the photo-polymerization of a composite resin. Fontes et al. [21] showed by multi-frequency EPR spectroscopy computational simulations, and DFT calculations that the EPR spectrum of the composite resin is formed by the superposition of the propagating radical (EPR signal with 9 lines) with the allylic radical (EPR signal with 5 lines).

As the polymerization reaction occurs independent of each initiation protocol and the closest neighbors of the unpaired electrons are the same as those found in the composite resin shown by Truffier-Boutry et al. and Fontes et al. [21, 22], it is to be expected that the X-band EPR spectrum of the resin cement has nine lines. Figure 6 shows the X-band EPR spectra of the photo-cured and the self-cured sample.

No significant differences between the spectra in Fig. 6 are noticed, and the spectra agrees with the one by Fontes et al. [21]. The nine-line EPR signal arises from the superposition of two radical species, a propagating radical with 9 lines and an allylic radical with five lines. To check for any other hidden radical species we measured the EPR spectra at higher frequencies. The advantage of measuring at higher frequencies is the improved resolution, which should assist in differentiating paramagnetic species. At Q-band (Fig. 7a) and W-band (Fig. 7b) EPR frequencies, the spectra for the self-cured and photo-cured samples both are again very similar, so that no other radical species are expected. In both frequency bands, the spectra of the dual cure resin cement again agree with those obtained by Fontes et al. [21], so that it is concluded, that the superposition model for the radicals is applicable to the polymerization reaction.

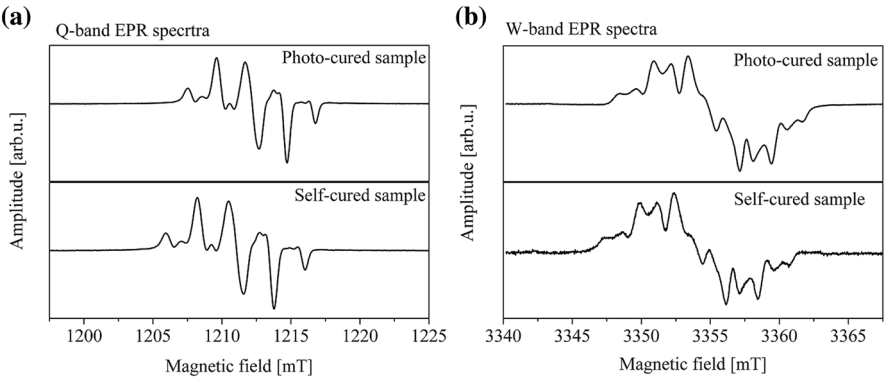

Fig. 7 EPR spectra for the photo-cured and the self-cured samples of the dual cure resin cement AllCem in **a** Q-band and **b** W-band

3.3 EPR Spectra Simulation

To verify if the proposed model of two different radicals is valid in this case and also check that the unpaired electrons interacts with similar neighbors independently the polymerization mode, EPR spectrum simulation in X-, Q- and W-band for both self-cured and phot-cured samples were performed.

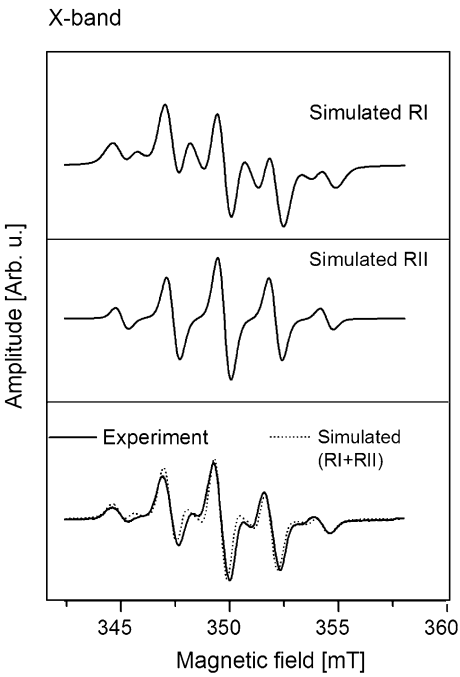

Fig. 8 EPR spectrum simulation for the self-cured sample in X-band. **a** The spectrum simulation for radical I. **b** The spectrum simulation for radical II. **c** Superposition of the experimental and simulated "radical I + radical II" spectra. The relative amounts of the two radicals are 10 and 90 %, respectively

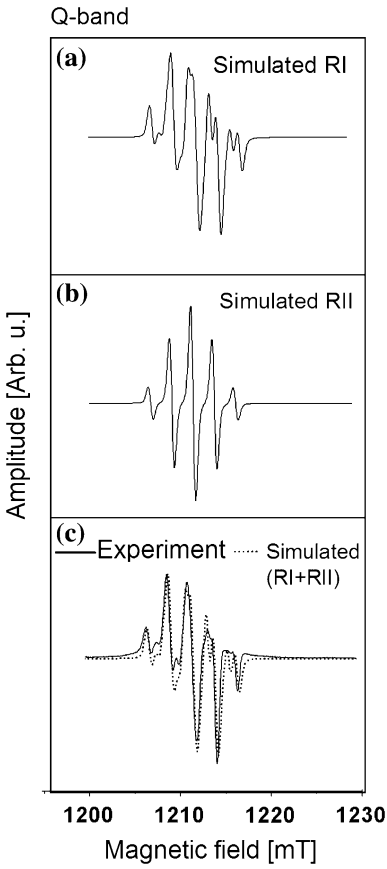

Fig. 9 EPR spectra simulation for the self-cured sample in Q-band. **a** The Q-band EPR spectrum simulation for radical I. **b** The Q-band EPR spectrum simulation for radical II. **c** Superposition of the experimental and simulated "radical I + radical II" spectra. The relative amounts of the two radicals are 10 and 90 %, respectively

The spin hamiltonian can be represented as $H_I = g\beta HS + [(AIa)IS + (AIb)IS + (AIc)IS]$ for propagating radical (CH_2-C*-CH_3), and $H_{II} = g\beta HS + [(AIIa)IS + (AIIb)IS]$ for allylic radical (CH_2-C*-CH_2), where gßHS is the Zeeman effect, AIa, AIb, and AIc are the hyperfine interactions coupling constants (hfcc) for radical I, and AIIa and AIIb are the hfcc for radical II. Here, we considered for radical I three equivalent protons of CH_3 group and two non equivalent protons of CH_2 group. For radical II we supposed two equivalent protons for each CH_2 group [21]. The relative amounts of the two radicals are 10 and 90 %, respectively [21].

Figures 8, 9 and 10 shows the results of spectrum simulation of self-cured sample in X-, Q- and W-bands. The parameters obtained by simulation for radical I and radical II are shown in Table 1. Table 2 shows values of spectroscopic parameters g and linewidth l.

We found that radical I is anisotropic while radical II is isotropic, and that the formation of EPR spectrum occur independently of the initiation mode. These

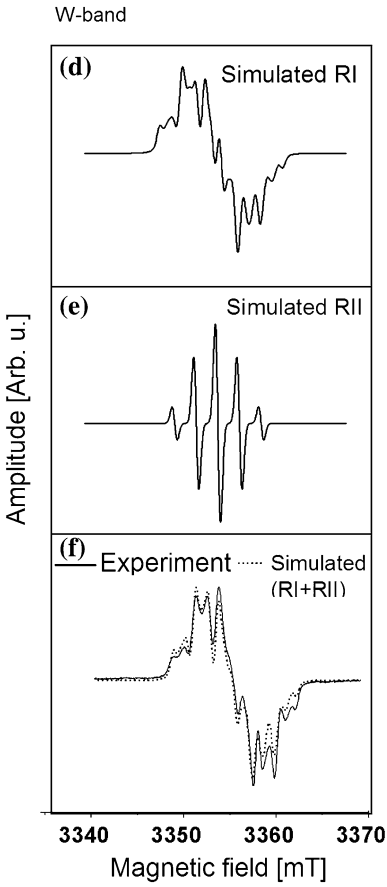

Fig. 10 EPR spectra simulation for the self-cured sample in W-band. **a** The W-band EPR spectrum simulation for radical I. **b** The W-band EPR spectrum simulation for radical II. **c** Superposition of the experimental and simulated "radical I + radical II" spectra. The relative amounts of the two radicals are 10 and 90 %, respectively

results are in accordance with Fontes et al. [21] for a photopolymerizable dental composite resin and confirms that the EPR signal arises from the superposition of two different radicals—propagating methacrylate radical (CH_2-C*-CH_3) and allylic radical (CH_2-C*-CH2)—for both self-cured and photo-cured sample, as the parameters obtained are the same. The model proposed is sufficient to explain the formation of the EPR spectrum in different frequencies.

4 Conclusions

It was possible to identify the free radicals responsible for the addition of monomers to the chain by multifrequency EPR spectroscopy and spectra simulation. It was concluded that there are two paramagnetic species forming

Table 1 Values of hfccs obtained by spectra simulation in X-, Q- and W-band of self-cure and photo-cure resin cement

	$AIa_x/g\beta$	$AIa_y/g\beta$	$AIa_z/g\beta$	$AIb_x/g\beta$	$AIb_y/g\beta$	$AIb_z/g\beta$	$AIc_x/g\beta$	$AIc_y/g\beta$	$AIc_z/g\beta$
Radical I hfccs (mT)									
Self-cured	2.32 ± 0.15	2.32 ± 0.16	2.33 ± 0.17	1.33 ± 0.06	1.60 ± 0.35	1.48 ± 0.10	0.92 ± 0.06	0.78 ± 0.06	0.89 ± 0.04
Photo-cured	2.32 ± 0.15	2.32 ± 0.16	2.33 ± 0.17	1.33 ± 0.06	1.60 ± 0.35	1.48 ± 0.10	0.92 ± 0.06	0.78 ± 0.06	0.89 ± 0.04
	$AIIa_x/g\beta$	$AIIa_y/g\beta$	$AIIa_z/g\beta$	$AIIb_x/g\beta$	$AIIb_y/g\beta$	$AIIb_z/g\beta$	–	–	–
Radical II hfccs (mT)									
Self-cured	2.28 ± 0.10	2.28 ± 0.10	2.28 ± 0.10	2.28 ± 0.10	2.28 ± 0.10	2.28 ± 0.10	–	–	–
Photo-cured	2.28 ± 0.10	2.28 ± 0.10	2.28 ± 0.10	2.28 ± 0.10	2.28 ± 0.10	2.28 ± 0.10	–	–	–

Table 2 Spectroscopic parameter *g* and linewidth obtained by spectra simulation in X-, Q- and W-band of self-cure and photo-cure resin cement

	g_x	g_y	g_z	l_x (mT)	l_y (mT)	l_z (mT)
Radical I						
Self-cured	2.0024 ± 0.0023	2.0034 ± 0.0015	2.0032 ± 0.0016	0.59 ± 0.00	0.59 ± 0.00	0.61 ± 0.03
Photo-cured	2.0024 ± 0.0023	2.0034 ± 0.0015	2.0032 ± 0.0016	0.59 ± 0.00	0.59 ± 0.00	0.61 ± 0.03
Radical II						
Self-cured	2.0030 ± 0.0018	2.0030 ± 0.0018	2.0030 ± 0.0018	0.55 ± 0.00	0.55 ± 0.00	0.55 ± 0.00
Photo-cured	2.0030 ± 0.0018	2.0030 ± 0.0018	2.0030 ± 0.0018	0.55 ± 0.00	0.55 ± 0.00	0.55 ± 0.00

the EPR spectrum, RI (CH3-C*-CH2) and RII (CH2-C*-CH2). The radical species are simultaneously present in the sample and occur independently of the polymerization protocol.

Acknowledgments We thank the EPR division of Bruker-BioSpin GmbH (Rheinstetten, Germany) for recording the spectra in W- and Q-band and FGM Produtos Odontológicos Ltda (Joinvile, SC, Brazil) for providing dental materials.

References

1. M.C. Cagidiaco, C. Goracci, F.G. Godoy, M. Ferrari, Int. J. Prosthodont. **21**, 328–336 (2008)
2. I.D. Sideridou, D.S. Achilias, O. Karava, Macromol. **39**, 2072–2080 (2006)
3. R.G. Craig, *Restorative Dental Materials*, 10th edn. (Mosby-Year Book Inc, St. Louis, 1997)
4. B.L.S. Vicentin, F.M. Salomão, M.G. Hoeppner, E. Di Mauro, Appl. Magn. Reson. **47**(2), 211–222 (2016)
5. F.M. Salomão, B.L.S. Vicentin, E.F.R. Contreras, M.G. Hoeppner, E. Di Mauro, Mater. Res. **18**(5), 1023–1028 (2015)
6. C. Moin Jan, Y. Nomura, H. Urabe, M. Okazaki, H. Shintani, J. Biomed. Mater. Res. B Appl. Biomater. **58**, 42–46 (2001)
7. J.L. Ferracane, E.H. Greener, J. Biomed. Mater. Res. **20**, 121–131 (1986)
8. J.L. Ferracane, J.C. Mitchem, J.R. Condon, R. Todd, J. Dent. Res. **76**, 1508–1516 (1997)
9. A. Peutzfeldt, E. Asmussen, J. Dent. **28**, 447–452 (2000)
10. L. Musanje, J.L. Ferracane, R.L. Sakaguchi, Dent. Mater. **25**, 994–1000 (2009)
11. H.F. Albers, *Tooth-Colored Restoratives: Principles and Techniques*, 9th edn. (BC Decker Inc., Hamilton, 2002)
12. D. Watts, N. Silikas, in *Dental Hard Tissues and Bonding—Interfacial Phenomena and Related Properties*, ed. by G. Eliades, D.C. Watts, T. Eliades (SpringerVerlag, Berlin, 2005)
13. L. Feng, B.I. Suh, J. Biomed. Mater. Res. B Appl. Biomater. **76**, 196–202 (2006)
14. H.W. Roberts, D.L. Leonard, K.S. Vandewalle, M.E. Cohen, D.G. Charlton, Dent. Mater. **20**(7), 617–622 (2004)
15. O. Yoldas, T. Alaçam, J. Endodon. **31**(2), 104–106 (2005)
16. F.R. Tay, R.J. Loushine, P. Lambrechts, R.N. Weller, D.H. Pashley, J. Endodon. **31**(8), 584–589 (2005)
17. C. Goracci, M. Ferrari, Aust. Dent. J. **56**(1), 77–83 (2011)
18. A. Marchi-Netto, J. Steinhaus, B. Hausnerova, B. Moeginger, B. Blümich, Appl. Magn. Reson. **44**(9), 1027–1039 (2013)
19. J. Leprince, G. Lamblin, D. Truffier-Boutry, S. Demoustier-Champagne, J. Devaux, M. Mestdagh, G. Leloup, Acta Biomate. **5**, 2518–2524 (2009)

20. L.G. Lovell, K.A. Berchtold, J.E. Elliott, H. Lu, C.N. Bowman, Polym. Adv. Technol. **12**, 335–345 (2001)
21. A.S. Fontes, B.L.S. Vicentin, D.F. Valezi, M.F. Costa, W. Sano, E. Di Mauro, Appl. Magn. Reson. **44**(9), 681–692 (2014)
22. D. Truffier-Boutry, X.A. Gallez, S. Demoustier-Champagne, J. Devaux, M. Mestdagh, B. Champagne, G. Leloup, J. Polym. Sci. A Polym. Chem. **41**(11), 1691–1699 (2003)
23. M.F. Ottaviani, A. Fiorini, P.N. Mason, C. Corvaja, Dent. Mater. **8**(2), 118–124 (1992)
24. D.S. Achilias, I. Sideridou, Macromol. **37**, 4254–4265 (2004)